Journal of Undergraduate Chemistry Research, **2021**, 20 (2), 34

FORMATION OF NAPHTHALENE-BIPHENYL EXCIPLEX FROM VAN DER WAALS COMPLEX BY VAPOR DEPOSITION ON Al_2O_3

Samantha C. Rosenhagen*, Cassidy C. Tran* and A.M. Nishimura†

Department of Chemistry, Westmont College, Santa Barbara, CA 93108

Abstract

Naphthalene and biphenyl were individually and as a bilayer, vapor deposited on a cryogenically cooled crystal of Al_2O_3. The surface was then heated and the temperature was linearly ramped through the desorption temperature of both naphthalene and biphenyl. A bilayer of biphenyl and naphthalene formed a van der Waals complex at the interface as evidenced by the fluorescence from the naphthalene-biphenyl exciplex. During the TPD, thermally induced mixing of naphthalene and biphenyl occurred that facilitated the formation of complex through the entire adlayer and the intensity of the exciplex increased to a maximum before desorption. The fluorescence spectra of the bilayer were acquired in real time during the mixing and the evolution of the surface dynamics was determined from the spectral signatures of the individual adsorbates. A plot of the intensity of the naphthalene-biphenyl exciplex as a function of the ratio of the coverages of biphenyl to naphthalene showed the stoichiometry of the exciplex is 1:1.

†corresponding author: nishimu@westmont.edu

Keywords: naphthalene, biphenyl, van der Waals complex, temperature programmed desorption, TPD, wavelength resolved TPD.

Introduction

Polycyclic aromatic hydrocarbons, PAH, have received attention in recent years because of their presence in the solar system (1-2) and in our atmosphere (3). The van der Waals complexes of PAH have been subjects of investigation both experimentally (4) and theoretically (5-6). Of interest in our laboratory is the van der Waals complex that potentially could form between naphthalene and biphenyl, especially if biphenyl is in the planar conformation.

Biphenyl itself is an interesting molecule because the dihedral angle between the two planar phenyl groups can vary (7-9). In the gas phase, the dihedral angle is about 45^o (3), whereas in the crystalline state at room temperature, the two rings are in a double minimum potential and statistically centered (8). The 45^o dihedral angle that is observed in the gas phase is the result of the competition between the steric hindrance and repulsive forces of the ortho-hydrogens on one hand and the π-electrons that can delocalize if the phenyl groups were co-planar (9).

The molecular fluorescence emission of biphenyl has been well documented (10-11). The spectral profiles of several substituted biphenyls in which the biphenyl was in the planar and out-of-plane conformers have been examined (12-13). The $\lambda_{max} \sim 320$ nm fluorescence has been assigned to the non-planar conformer of biphenyl and the $\lambda_{max} \sim 345$ fluorescence has been assigned to the planar conformer (12-13). When vapor deposited on Al_2O_3 at 138 K, the amorphous planar conformer predominate and has a $\lambda_{max} \sim 370$ nm (13-14). This has been assigned to the planar biphenyl in the biphenyl excimer (12-14).

In addition he conformer of biphenyl in an adlayer will vary, depending on the nature of the underlayer (15). The planar conformer of biphenyl can be formed either by deposition at 138 K or by epitaxy on top of a naphthalene underlayer. Emission from either 345 or 370 nm would confirm planar biphenyl and possible naphthalene-biphenyl complex. With this distinction in mind, both molecules were vapor deposited in search of the van der Waals complex and the resulting fluorescence from the exciplex.

Experimental

Biphenyl and naphthalene were of the highest purity that were commercially available, > 99% (Sigma-Aldrich, St. Louis, MO). These compounds were placed in separate sample holders, outgassed and introduced into the ultra-high vacuum chamber with background base pressure of 1×10^{-9} torr. Deposition onto a single crystal of Al_2O_3 (0001) (Crystal Systems, Inc., Salem, MA) was accomplished from the vapor through variable leak valves. The substrate was suspended on the end of a liquid nitrogen cryostat via copper post on either side of the Al_2O_3 with a sapphire spacer for electrical and thermal isolation. Resistive heating of the Al_2O_3 was done by sending current through a thin tantalum foil that was in thermal contact with the substrate. A type-K thermocouple that was also in thermal contact with the Al_2O_3 monitored the temperature.

Details of the experimental set up have been previously published (15) and a brief summary is given here. During the TPD, a LabVIEW (National Instruments, Austin, TX) program was written in-house was used to take the fluorescence spectra from the Ocean Optics USB4000 spectrometer (Ocean Optics, Dunedin, FL) in real time every 300 ms. The program simultaneously monitors the surface temperature of the Al_2O_3 crystal, and via a PID (proportional-integral-derivative) feedback algorithm, linearly increments the temperature of the Al_2O_3 crystal in the TPD experiments. The program also scans the residual gases analyzer that detects the desorption of gases from the Al_2O_3. Manipulation of the array of spectra as a function of temperature by a MATLAB (Mathworks, Natick, MA) template yielded the wavelength resolved TPD's that are shown in the figures. To ensure a clean surface, the Al_2O_3 was heated to 300 K after each run.

The activation energy for desorption, E_a, was calculated by Redhead analysis in which a first-order desorption kinetics as described by King was assumed and is based on the mass spectral peak desorption temperature, T_p (16-18). The uncertainties in the desorption temperatures and the propagated error in the activation energies were ± 2%.

The surface coverages, Θ, in monolayers (ML) were calculated by calibrating the integrated mass spectral peak areas to an optical interference experiment. The interference experiment yielded accurate rate of deposition with coverage error of ± 30%, and is described in detail elsewhere (15).

Results and Discussion

Biphenyl:

The peak desorption temperature, T_p, of neat biphenyl was 234 K. First-order desorption was assumed and the activation energy for desorption, E_a, was calculated to be 60.8 kJ/mol (16-18). Upon deposition, excitation of neat biphenyl on the Al_2O_3 surface with a high-pressure Hg lamp centered at 250 nm caused the amorphous biphenyl to fluoresce with a λ_{max} of 320 nm. This fluorophore has been assigned to the twisted conformer of biphenyl (12-13). As can be seen from Figure 1, when the surface temperature was linearly ramped, the adlayer underwent a disorder-to-order transition at 160 K, where λ_{max} red-shifted to 345 nm. This fluorophore has been assigned to the planar conformer of biphenyl (12-13). The reduction in intensity by about 30% occurred from the ordered molecules that became energy carriers to the trap sites from which radiative relaxation occurred (13).

Naphthalene:

For aromatic molecules, vacuum deposition typically prepares them in an amorphous state in which molecules are on the average sufficiently close such that upon excitation, two nearest neighbor molecules transiently stack to form the excimer (10-11). Then, when the surface temperature is ramped up in a TPD experiment, the adlayer undergoes a disorder-to-order transition, whereupon the emission changes from excimer to molecular fluorescence from trap sites due to the ordering that occurs (13). In polyaromatic molecules, the molecular fluorescence is characterized by λ_{max} that is blue-shifted from that of the excimer fluorescence (11). For example, the blue-shift in λ_{max} from excimer to molecular fluorescence for naphthalene and substituted naphthalenes corresponds to ~ 50 kJ/mol of energy (13).

Figure 2 shows the wavelength-resolved TPD of naphthalene. The fluorescence spectrum as a function of temperature was dominated by excimer fluorescence with λ_{max}~ 397 nm. The peak desorption temperature for naphthalene was 215 K. A first-order desorption kinetics was assumed and E_a was calculated to be 55.8 kJ/mol (16-18). Naphthalene underwent a disorder-to-order transition at beginning at 160 K with a fluorescence λ_{max}~ 325 nm with an accompanying peak at λ_{max}~ 334 nm due to the C-H bending motion. These peaks due to the monomer had very low intensities and are difficult to see in the figure.

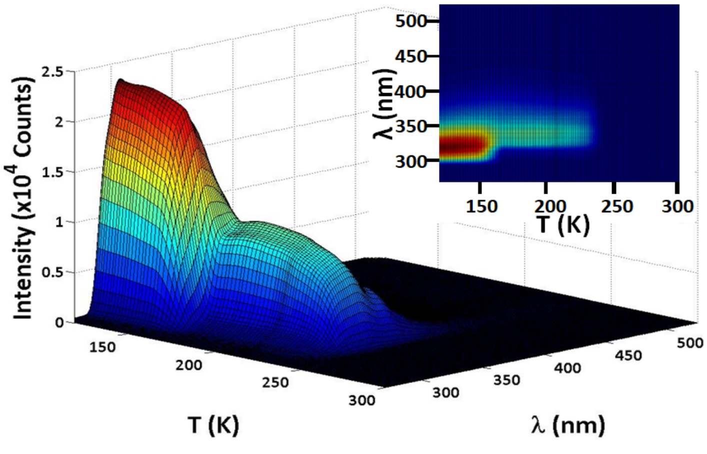

Figure 1. Wavelength-resolved TPD of multilayer biphenyl. $\Theta_{biphenyl}$ = 340 ML. Biphenyl deposited in the twisted conformation with λ_{max} ~ 320 nm that red-shifts to 340 nm subsequent to the disorder-to-order transition. Inset: top view.

Bilayer of naphthalene and biphenyl:

Shown in Figure 3 is the wavelength-resolved TPD of the bilayer of biphenyl and naphthalene in which biphenyl with the higher T_p was deposited first. Note that the fluorescence due to the two individual adsorbates can be distinguished for naphthalene from Figure 2 and for biphenyl from Figure 1. Clearly, the mixing does not occur until about 215K, or about 20 K prior to desorption. Additionally, the surface created by the biphenyl adlayer that was deposited first was roughly like that of Al_2O_3, since the fluorescence TPD of naphthalene was similar to that observed in Figure 2.

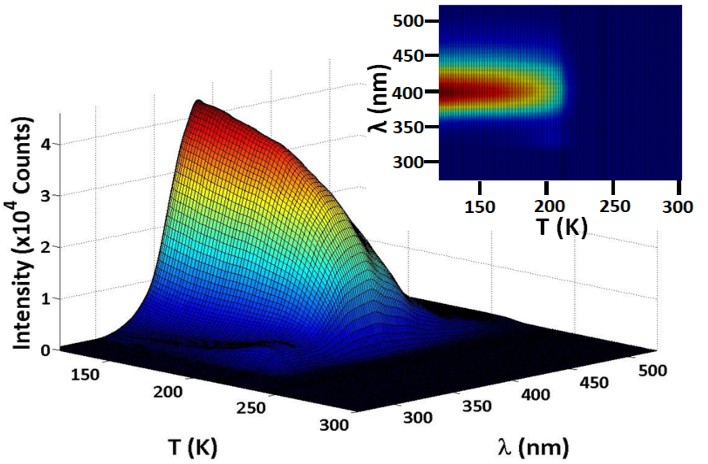

Figure 2. Wavelength-resolved TPD of multilayer naphthalene $\Theta_{naphthalene}$ = 120 ML. The excimer fluorescence at λ_{max} ~ 395 nm dominate at deposition that blue-shifts to 325 nm subsequent to the disorder-to-order transition. Inset: top view.

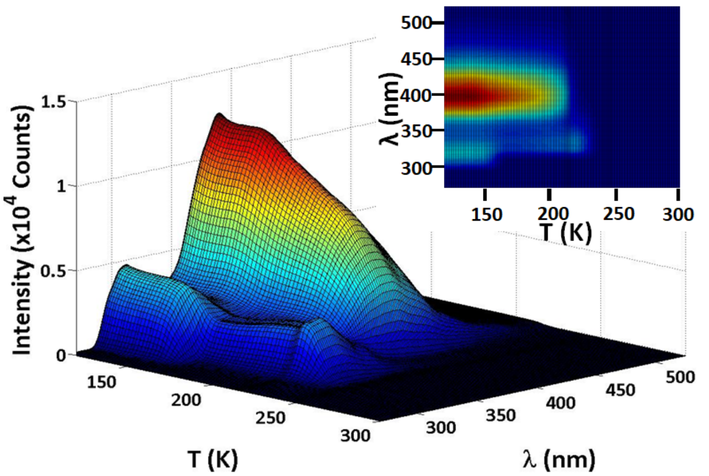

Figure 3. Wavelength-resolved TPD of bilayer of biphenyl and naphthalene for which $\Theta_{biphenyl}$ = 140 ML and $\Theta_{naphthalene}$ = 140 ML. The fluorescence from the two adsorbates are distinguishable. Mixing occurs at about 20 K before desorption. Inset: top view.

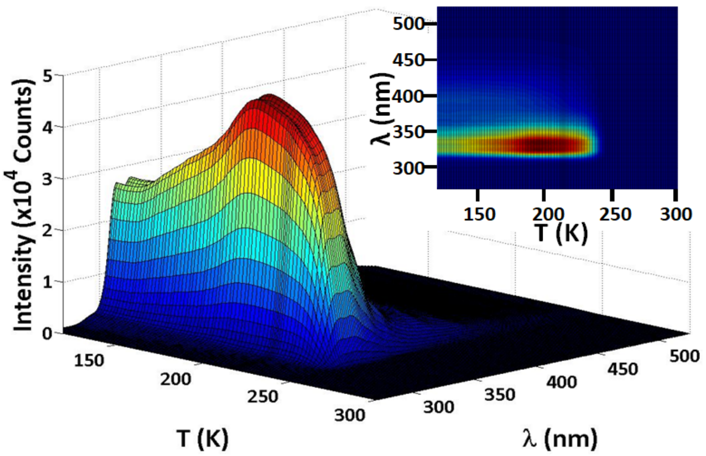

Figure 4. Wavelength-resolved TPD of bilayer of naphthalene and biphenyl, for which $\Theta_{\text{naphthalene}}$ = 140 ML and Θ_{biphenyl} = 440 ML. The fluorescence is that of molecular naphthalene with λ_{max} ~ 325 and 334 nm. Note the absence of the 320 nm emission from the twisted conformer of biphenyl. Inset: top view. The excimers of biphenyl and naphthalene are barely visible at 370 and 397 nm, respectively.

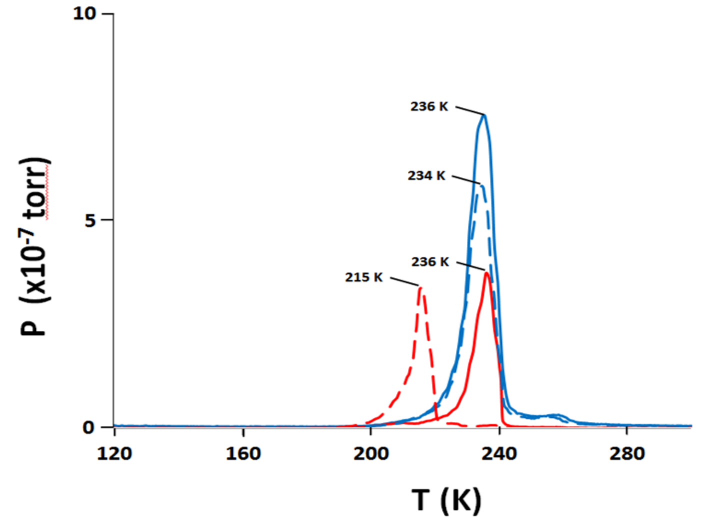

Figure 5. Mass specific TPD for multilayer biphenyl, multilayer naphthalene and biphenyl and naphthalene in the bilayer. T_p's for pure naphthalene (red, dashed plot) and pure biphenyl (blue, dashed plot) are 215 and 234 K, respectively. In the bilayer, T_p's for naphthalene (red, solid plot) and biphenyl (blue, solid plot) are both 236 K.

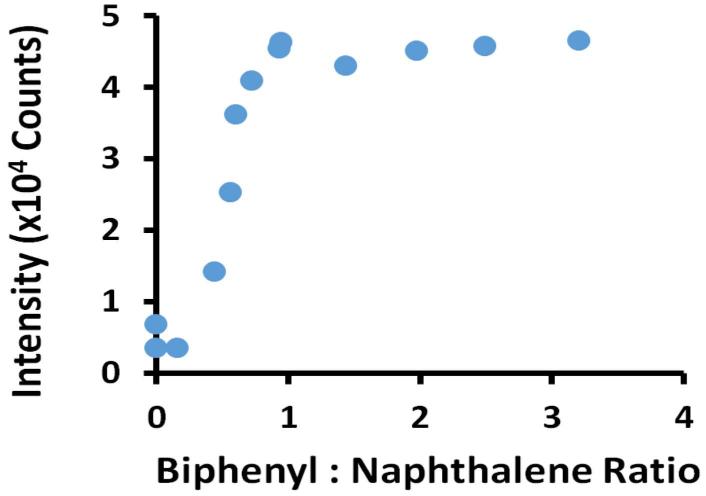

Figure 6. Maximum Intensity of the naphthalene peaks at 325 and 334 nm at T = 210 K in Figure 4 as a function of the ratio of biphenyl to naphthalene coverages. $\Theta_{\text{naphthalene}}$ was held constant at 146 ± 14 ML.

Shown in Figure 4 is the bilayer of naphthalene on the bottom and biphenyl on top in which the coverages were $\Theta_{\text{naphthalene}}$ = 140 ML and Θ_{biphenyl} = 440 ML, respectively. Here the spectrum is sufficiently resolved to assign the two peaks at λ_{max} ~ 325 and 334 nm to molecular naphthalene. Careful examination of the spectra upon deposition of the bilayer of naphthalene and biphenyl revealed the absence of the biphenyl in the twisted conformer, but instead, presence of a broad peak at λ_{max} ~ 370 nm was observed that was assigned to the biphenyl excimer. Therefore biphenyl is epitaxially in the planar conformation when deposited onto the naphthalene adlayer (12-14). The intensities of both the naphthalene excimer and biphenyl excimers were highly attenuated from those observed for neat naphthalene (Figure 2) and biphenyl (Figure 1) at similar coverages. On the other hand, the surprising large *initial* fluorescence intensity is evidence of the naphthalene-biphenyl exciplex which is formed. (Figure 4). This observation led to the hypothesis that the surface of naphthalene is very rough and the van der Waals sufficiently large so that a significantly large number of biphenyl molecules can be accommodated.

Additional evidence for the formation of van der Waals complex was deduced from the mass spectral data. As shown in Figure 5, multilayer naphthalene and biphenyl desorbed at 215 K (E_a = 55.8 kJ/mol) and at 234 K (E_a = 60.8 kJ/mol), respectively. In the bilayer study with the naphthalene deposited first, biphenyl and naphthalene desorb *together* at 236 K (E_a = 61.2 kJ/mol). The shift in the desorption energy of 5.4 ±0.2 kJ/mol for naphthalene is a rough estimate of this van der Waals interaction energy.

The maximum fluorescence intensities of the bilayer at λ_{max} ~ at 325 and 334 nm that occurred during the TPD at about 210 K in Figure 4 were plotted as a function of the ratio of coverages: Θ_{biphenyl} to $\Theta_{\text{naphthalene}}$ (ML/ML) are shown in Figure 6. The maximum intensity of the naphthalene peaks leveled at a monolayer ratio of ~ 1:1 (ML/ML) and would be a reasonable stoichiometric ratio for the complex. In this study the naphthalene was held constant at $\Theta_{\text{naphthalene}}$ ~ 146 ± 14 ML.

In summary, when naphthalene is deposited on Al_2O_3, its surface is sufficiently rough that when biphenyl is vapor deposited on it, a van der Waals dimer (with a 1:1 stoichiometry) forms with biphenyl in the planar conformer. Since the twisted conformer of biphenyl is absent, naphthalene serves as a good underlayer for the biphenyl to deposit in the planar conformation.

Acknowledgement

The authors would like to thank the John Stauffer Charitable Trust for funding the student stipends for summer research.

References

(1). L. Zhao, R.I. Kaiser, B. Xu, U. Ablikim, M. Ahmed, M. Evseev, E.K. Bashkirov, V.N. Azyazov and A.M. Mebel. *Nature Astronomy*, **2018**, 2, 973-979.

(2). L. Biennier, H. Sabbah, V. Chandrasekaran, S.J. Klippenstein, I.R. Sims and B.R. Rowe, *Astronomy and Astrophysics*, **2011**, 432, 1-7.

(3). K. Ravindra, R. Sokhi and R. Van Grieken. *Atmospheric Environment*, **2008**, 42, 2895-2921.

(4). A. Kas, C.K. Nandi and T. Chakraborty, *J. Chem Phys*., **2003**, 118, 9589-9595.

(5). S.D. Chakarova and E. Schröder. *J. Chem. Phys*., **2005**, 122, 54102.

(6). N.K. Lee, S. Park and S.K. Kim. *J Chem Phys*., **2002**, 116, 7902.

(7). A. Almenningen, O. Bastiansen, L. Fernholt, B.N. Cyvin, S.J. Cyvin and S. Samdal. *J. Mol. Struct.*, **1985**, 128, 59-76.

(8). G.P. Charbonneau and Y. Delugeard. *Acta Crystallographica B*, **1976**, 32, 1420-1423.

(9). G. Friedrich. *J. Phys. Chem. A*, **2002**, 106, 3823-3827.

(10). I.B. Berlman. Handbook of Fluorescence Spectra of Aromatic Molecules, 2nd edition, Academic Press, New York, NY (1971) pp.176-177,330.

(11). J.B. Birks. Photophysics of Aromatic Molecules, John Wiley & Sons Ltd., New York, NY (**1970**), pp. 301-370.

(12). Marissa K. Condie, Zackery E. Moreau and A.M. Nishimura. *J. Undergrad. Chem. Res.*, **2019**, 18, 15-18.

(13). B.D. Fonda, M.K. Condi, Z.E. Moreau, Z.I. Shih, B. Dionisio, A. Fitts, L. Foltz, K. Nili and A.M. Nishimura. *J. Phys. Chem. C.*, **2019**, 123, 26185-26190.

(14). M.K. Condie, C. Kim, Z.E. Moreau, B. Dionisio, K. Nili, J. Francis, C. Tran, S. Nakaoka and A.M. Nishimura. *J. Undergrad. Chem. Res*., **2020**, 19, 14-17

(15). M.K. Condie, B.D. Fonda, Z.E. Moreau and A.M. Nishimura. *Thin Solid Films*, **2020**, 697, 137823.

(16). P.A. Redhead. *Vacuum*, **1962**, 12, 203-211.

(17). F.M. Lord and J.S. Kittelberger. *Surf. Sci.*, **1974**, 43, 173-182.

(18). D.A. King. *Surf. Sci.,* **1975***,* 47, 384-402.